International Journal of Mass Spectrometry 308 (2011) 338–347

Contents lists available at SciVerse ScienceDirect

International Journal of Mass Spectrometry

journal homepage: www.elsevier.com/locate/ijms

Structure of singly hydrated, protonated phospho-tyrosine

D. Scuderi[a], J.M. Bakker[a,1], S. Durand[a], P. Maitre[a,*], A. Sharma[b], J.K. Martens[b], E. Nicol[b], C. Clavaguéra[b,*], G. Ohanessian[b,*]

[a] Laboratoire de Chimie Physique, Université de Paris-Sud 11, CNRS, 91405 Orsay Cedex, France
[b] Laboratoire des Mécanismes Réactionnels, Ecole polytechnique, CNRS, 91128 Palaiseau Cedex, France

ARTICLE INFO

Article history:
Received 24 June 2011
Received in revised form 26 August 2011
Accepted 31 August 2011
Available online 9 September 2011

Keywords:
IRMPD spectroscopy
Phosphorylated aminoacids
Phosphorylated tyrosine
Microsolvation
Microhydration
Quantum chemistry
DFT
MP2

ABSTRACT

Tandem mass spectrometry is a powerful analytical technique for distinguishing phosphorylated from non-phosphorylated peptides, and also to locate the phosphorylated site. It is however desirable to further extend the tandem MS capacities via the development of structure specific activation techniques. This work is part of an ongoing project which aims at characterizing the environment of the phosphate group using tunable IRMPD. The effect of microsolvation of protonated phospho-tyrosine on the phosphate environment has been investigated using a combination of tandem MS experiments and quantum chemical calculations. Infrared spectra have been recorded in the 900–1900 cm^{-1} and 2500–3750 cm^{-1} regions using a free electron laser and a tabletop laser, respectively. Water is found to form a hydrogen bonded bridge between the otherwise nearly isolated phosphate and ammonium groups. Theoretical and experimental results also provide consistent evidences for two weaker hydrogen bonds between the two other NH bonds with the π-aromatic ring and the carboxylic CO. The MP2 calculated IR absorption spectrum of the lowest energy structure allows for a clear band assignment. As compared to intramolecular direct interaction between the phosphate and the ammonium, the two hydrogen bonds associated with the water bridge between these groups are found to have a larger impact on their IR structure-specific probes. This is reflected by the red-shift of the P═O stretch, and also the blue shift of the umbrella mode of the ammonium. Special attention is paid to the 2500–3750 cm^{-1} spectral range. While the phosphate OH stretching modes are not affected by the addition of water, the red shifts of the three ammonium NH stretches are found to be significant and quite different for their three types of non-covalent interactions.

1. Introduction

Reversible phosphorylation of the alcohol on the side chain of serine (Ser), threonine (Thr) or tyrosine (Tyr) residues is among the most frequent post-translational modifications (PTM) of proteins. Several thousand sites of post-translational phosphorylation are now known, and estimates of the fraction of proteins that are phosphorylated *in vivo* are as high as 30% [1]. Protein phosphorylation often leads to considerable conformational changes [2] and these changes are likely to be part of the impact that phosphorylation is known to have on protein function. It is therefore of crucial importance to develop techniques to detect, locate, and structurally characterize these modifications in peptides and proteins.

Mass spectrometric techniques have proven to be powerful tools for the identification and analysis of phosphorylated peptides [3]. Tandem mass spectrometry provides sequence information for library-based protein identification and the determination of post-translational modifications. It allows the detection of phosphorylated sites based on the loss of characteristic neutral fragments (−80 Da (HPO_3) and/or −98 Da (H_3PO_4) in positive ion MS/MS) [4]. It is usually carried out using Collision Induced Dissociation (CID) to activate and fragment ions. It is worth noting, however, that several studies have shown that InfraRed Multiple Photon Dissociation (IRMPD) at fixed-wavelength (10.6 μm) using a CO_2 laser is also very interesting for distinguishing phosphorylated from non-phosphorylated peptides [5]. The former can be selectively fragmented since the CO_2 laser is resonant with one or more phosphate POH vibrational modes, leading to a much more efficient fragmentation of phosphorylated peptides than non-phosphorylated ones. Thus IRMPD at fixed-wavelength (10.6 μm) provides an easy way to characterize which peptides are phosphorylated within a complex mixture. This has been achieved in both negative [5] and positive [6] ion modes. In addition, the output of a CO_2 laser is powerful enough

* Corresponding authors.
E-mail addresses: philippe.maitre@u-psud.fr (P. Maitre), carine.clavaguera@dcmr.polytechnique.fr (C. Clavaguéra), gilles.ohanessian@polytechnique.fr (G. Ohanessian).
[1] Current address: FOM Institute for Plasmaphysics, Rijnhuizen, Edisonbaan 14, NL-3439 MN Nieuwegein, The Netherlands.

1387-3806/$ – see front matter © 2011 Elsevier B.V. All rights reserved.
doi:10.1016/j.ijms.2011.08.031

that multiple sequential fragmentations can be easily generated to yield rich sequence information in a single experiment [6].

A step forward in structural determination using IRMPD can be taken by using tunable infrared lasers [7]. Compared to commonly used IRMPD with fixed-wavelength CO_2 lasers, free electron lasers (FEL) and OPO/OPA lasers provide access to a wide frequency range [8], enabling to record vibrational spectra in the mid-infrared and in the N–H/O–H stretching regions. This has the potential for distinguishing between isomers as in the case of glucose-containing disaccharides [9], and in certain cases between conformers of sodiated oligopeptides [10], for example. In a previous paper, we obtained the IRMPD signatures of the three protonated, phosphorylated amino acids: phospho-serine ($pSerH^+$), phospho-threonine ($pThrH^+$) and phospho-tyrosine ($pTyrH^+$) [11]. The results indicated that phosphate specific bands exist as expected and that they are easily detectable in IRMPD conditions. Detailed band assignment based on quantum chemical calculations established that some features were common to all three species, while others were specific. Among the latter, the C–OP stretch of the phosphate ester was found to be very different in $pSerH^+$ and $pThrH^+$ on one hand, and in $pTyrH^+$ on the other. The difference lies in the aliphatic vs aromatic character of the carbon atom, and in additional coupling of C–OP stretch with aromatic CCH bends for $pTyrH^+$. Thus this band can be used as an intrinsic signature of $pSerH^+$ or $pThrH^+$ vs $pTyrH^+$. Furthermore, a second distinction was established, in which it is the environment that is distinctive. As discussed previously [11], the most favorable protonation site is the amine in all three cases, leading to primary ammonium groups in the protonated species. In $pTyrH^+$, the amino acid and phosphate moieties are held apart by the benzyl group of the tyrosine side chain. As a result, the P=O bond can interact with the amino acid only weakly at most. In $pSerH^+$ and $pThrH^+$, hydrogen bonding can be established between the ammonium and the phosphate. This interaction results in a red shift of ca. 50 cm^{-1} for the P=O stretch with respect to the free P=O stretching frequency (1265 cm^{-1}) for $pTyrH^+$ [11]. This band may thus be used as a probe of the environment of the P=O bond. Similar work has been described for deprotonated, phosphorylated amino acids [12].

These results indicate that some of the phosphate vibrational modes, as well as those of groups that interact with the phosphate, may be used as sensitive structural probes. Confirmation was obtained by recording the IRMPD spectrum of the phosphorylated dipeptide $GlypTyrH^+$ [13]. In this case, the G residue at the N terminus side of pTyr enables direct interaction of the terminal ammonium with the phosphate, leading to P=O stretch and ammonium umbrella frequencies that are similar to those in $pSerH^+$, while the C–OP stretch of the phosphate ester remains at the same frequency as in $pTyrH^+$.

In the present work we consider yet another environment change made to $pTyrH^+$ by micro-hydrating it with a single water molecule. Water is expected to bind most strongly to the charged site, which is very likely to be the amine. If it is able to bridge between the protonated amine and the phosphate groups, it will bring about a different type of perturbation to the phosphate P=O stretching motion. In order to obtain a more complete structural determination via IRMPD spectroscopy, we use two different experimental setups in order to record vibrational spectra in both the fingerprint and in the N–H/O–H stretching regions. The present results can then be compared to those described previously for $TyrH^+$ [14], $TyrAlaH^+$ and $AlaTyrH^+$ [15] and for $ValH^+(H_2O)$ [16] for which spectra have been described in the N–H/O–H stretching region. This extends to phosphorylated compounds the significant body of data already available in this spectral range.

2. Experimental and computational details

Experiments are performed employing a 7 Tesla FT-ICR mass spectrometer (Bruker, Apex Qe) coupled with infrared laser sources. A detailed layout of this experimental apparatus is described elsewhere [8,17]. Mass-selected ions are stored in the ICR cell where they are irradiated with the IR light. IR action spectroscopy is achieved by monitoring the parent and multiple fragments abundances (I_P and I_F, respectively) as a function of the laser wavelength. Spectra presented here correspond to IR photodissociation efficiency defined as $-\ln[I_P/(I_P + I_F)]$, where I_P and I_F are the intensity of the precursor ion and the sum of intensities of fragment ions, respectively, as a function of the laser wavelength. For each wavelength, the mass spectrum is the Fourier transform of a time-domain transient signal averaged 5–10 times.

Ions are generated by electrospray (ESI), and the ESI conditions used are as follows: flow rates of 60–80 μL/h and spray voltages of 4700–5000 V with a drying gas temperature of 150 °C. Phosphorylated tyrosine (pTyr) from Sigma–Aldrich was used without purification. One millimolar pTyr solutions were prepared by combining 100 μL of pTyr stock solution (10 mM), 1.0 mL of H_2O/MeOH 50:50, and 20 μL of formic acid 98%. Similar experimental conditions were used for benzylamine ($C_6H_5CH_2NH_2$).

The Bruker Apex Qe mass spectrometer features a quadrupole–hexapole interface between the electrospray source and the ICR cell. The desired ions are thus mass selected in the quadrupole, and are then trapped in a hexapole contained within a collision cell. Mass-selected ions are thus collisionally thermalized using a flow of high-purity argon buffer gas. Ions are then pulse-extracted towards the ICR cell where they are then irradiated with IR light, after which the resulting ions are mass-analyzed. This procedure was used for both protonated phosphorylated tyrosine ($pTyrH^+$) and protonated benzylamine ($C_6H_5CH_2NH_3^+$). Alternatively, if water is seeded in the buffer gas, water clustering can be observed [17–19]. In the case of protonated phospho-tyrosine ($pTyrH^+$), a substantial amount of mono-hydrated ions $pTyrH^+(H_2O)$ can be produced. These ions are then mass-selected in the ICR cell prior to their irradiation.

IR spectra of the cluster ions were recorded in the 2400–3800 cm^{-1} range using an optical parametric oscillator/amplifier (OPO/OPA from LaserVision, Bellevue, WA, USA) laser system. This laser system is pumped by an Innolas Spitlight 600 (München, Germany) non-seeded Nd:YAG (1064 nm, 550 mJ/pulse, bandwidth ~1 cm^{-1}) laser running at 25 Hz and delivering pulses of 4–6 ns duration. Typical output energy of the OPO/OPA was 12–13 mJ/pulse at 3600 cm^{-1} with a 3–4 cm^{-1} (fwhm) bandwidth. Infrared spectroscopy in the 800–2000 cm^{-1} spectral range was carried out using the free electron laser (FEL) at CLIO [20]. This FEL delivers so-called macropulses, typically ~8 μs long, at 25 Hz, which consist of a train of 0.5–6 ps (adjustable) micropulses. The micropulses are spaced by 16 ns. The typical IR FEL average power is 500 mW, which corresponds to micropulse and macropulse energies of 40 μJ and 20 mJ, respectively. In both cases, the IR laser beam is steered into the FT-ICR along the axis of the magnetic trapping field and loosely focused using a spherical mirror with a 2-m focal distance. The light beam has a nearly constant diameter throughout the ICR cell region [8].

To aid in interpretation of the recorded spectra, quantum chemical calculations are performed to identify the low energy structures of the molecular ions of interest and to compute their linear absorption spectra. The MP2/SVP level has been found to yield accurate results in the entire spectral range provided that frequencies are scaled by a factor of 0.943 [21]. It is however well documented that phosphate modes require a factor closer to 1 than do other modes in the fingerprint range [21]. One way to include this constraint could have been to use a specific factor for phosphate modes. This is

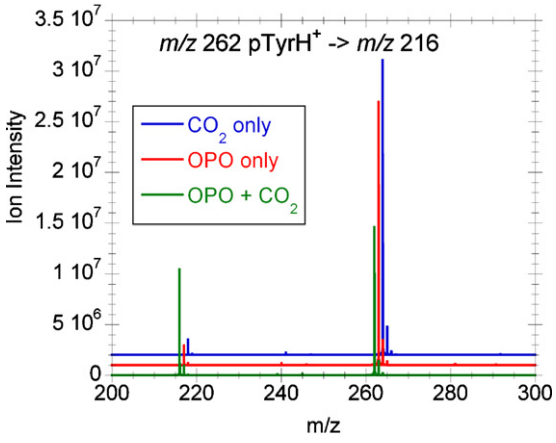

Fig. 1. IR-induced fragmentation mass spectra of $pTyrH^+$ using only the OPO/OPA on resonance at 3660 cm^{-1} (red), using the CO_2 laser and the OPO/OPA on resonance at 3660 cm^{-1} (green), and using only the CO_2 laser (blue). (For interpretation of the references to color in this figure legend, the reader is referred to the web version of the article.)

made difficult, however, by the water bridge in $pTyrH^+(H_2O)$ which induces significant mode delocalization over the phosphate and amino acid parts. The best compromise found is to use the standard factor of 0.943 in the 2900–4000 cm^{-1} range and a compromise factor of 0.96 for all frequencies below 2000 cm^{-1}. Additional calculations were carried out using various density functionals in an effort to calibrate their performances. The dispersion-corrected B3LYP-D hybrid density functional [22] and the hybrid M06 functional [23] were used associated with SVP and 6-31G(d,p) basis set, respectively. Calculations were performed using the Gaussian09 [24] and Turbomole 6.3 [25] program suites.

3. Results and discussion

3.1. Experimental IRMPD spectra

3.1.1. Mass spectra – fragmentation channels

Upon resonant IR activation, fragmentation of $pTyrH^+(H_2O)$ ions (*m/z* 280) is observed. For short irradiation time using the OPO/OPA laser, only the loss of the water molecule is observed. The subsequent fragmentation of the resulting $pTyrH^+$ (*m/z* 262) ions could be observed for longer irradiation time. The corresponding fragment ion (*m/z* 216) may result from the elimination of H_2O and CO [26]. In order to minimize saturation effects using the highly intense IR FEL, the irradiation time was set to 100 ms (i.e. two macropulses) to record the IR fingerprint spectrum of $pTyrH^+(H_2O)$. Using the less intense OPO/OPA laser system, the same irradiation time could be used for $pTyrH^+(H_2O)$. For the more strongly bound $pTyrH^+$ system, however, IR induced fragmentation was more difficult to achieved, especially in the NH stretching region where the OPO/OPA laser power is significantly lower. The $pTyrH^+$ (*m/z* 262) ions were irradiated for 3 s, and the OPO/OPA laser system was reoptimized for this spectral range. Alternatively, the IR spectrum of $pTyrH^+$ ions in the 3050–3400 cm^{-1} region could also be recorded using the OPO/OPA laser in combination with a broadband CO_2 laser (BFI Optilas) in order to enhance the photofragmentation yield of these strongly bound ions. As described elsewhere [19], the auxiliary CO_2 laser was used in a pulsed mode. A 7 ms long CO_2 pulse followed each OPO/OPA pulse, delayed by ~1 μs. Using this combination of two lasers, the irradiation time was set to 500 ms. Three fragmentation mass spectra of $pTyrH^+$ (*m/z* 262) are given in Fig. 1. As can be seen in this Figure, while ~5% fragmentation can be achieved using solely the OPO/OPA laser tuned on resonance at ~3660 cm^{-1}, a significant enhancement of the fragment signal (~73% of that of the parent ion) can be achieved using the auxiliary CO_2 laser. In the present case, the irradiation time was set to 500 ms.

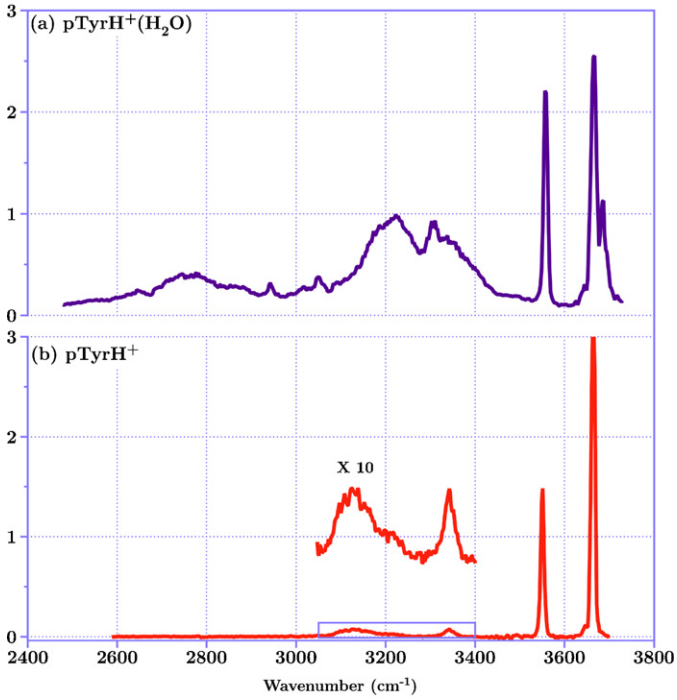

Fig. 2. IR photodissociation spectra of $pTyrH^+(H_2O)$ (a, top) and of $pTyrH^+$ (b, bottom) recorded in the X–H (X = C, N, O) stretching region.

3.1.2. IRMPD spectra

IR spectra in the 2400–3800 cm^{-1} spectral range of $pTyrH^+$ and $pTyrH^+(H_2O)$ are given in Fig. 2. As can be seen in this figure, relatively narrow spectral features can be observed in the higher frequency range, whereas below 3500 cm^{-1} the most intense IR bands are significantly broader. On the basis of the X–H (X = C, N, O) stretching frequencies reported in the literature, some spectral assignment can be made.

The narrow band (fwhm = 12 cm^{-1}) observed at 3552 and 3558 cm^{-1} for $pTyrH^+$ and $pTyrH^+(H_2O)$, respectively, is likely to be the signature of a free carboxylic OH. This vibrational mode was shown to be characterized with a very similar frequency value (ca. 3560 cm^{-1}) in the cases of protonated tyrosine [14] and hydrated protonated valine [16], for example. A second narrow band (fwhm = 12 cm^{-1}) is observed at about the same frequency (~3666 cm^{-1}) for $pTyrH^+$ and $pTyrH^+(H_2O)$. Given the assignment of the carboxylic CO–H stretch above, this can only be attributed to the phosphate PO–H stretches. This spectral assignment is further supported by the fact that in a study of the photolysis products of phosphine–ozone complexes isolated in solid Argon, a band observed at a similar position (3634.8 cm^{-1}) was assigned to the PO–H stretch of $(O{=}PH(OH)_2$ [27].

In the case of $pTyrH^+(H_2O)$ on the blue-side of, and slightly overlapping with the band at ~3666 cm^{-1} one can clearly distinguish a band centered at ~3686 cm^{-1} which is likely to be the signature of one of the water OH stretches. On the basis of the reported OH stretching frequencies of $NH_4^+(H_2O)_{2-8}$ clusters [28], this assignment is consistent with a water molecule that simultaneously acts as a hydrogen bond donor (D) and acceptor (A). Indeed an IR feature at 3688 cm^{-1} was assigned to free OH stretch of such a DA water in $NH_4^+(H_2O)_{6-7}$ [28]. For larger size $NH_4^+(H_2O)_{5-22}$ clusters [29], it has been shown that sharp free OH stretching bands centered around 3700 cm^{-1} provide the most structural information, and these bands were assigned to free OH stretching vibration of DA

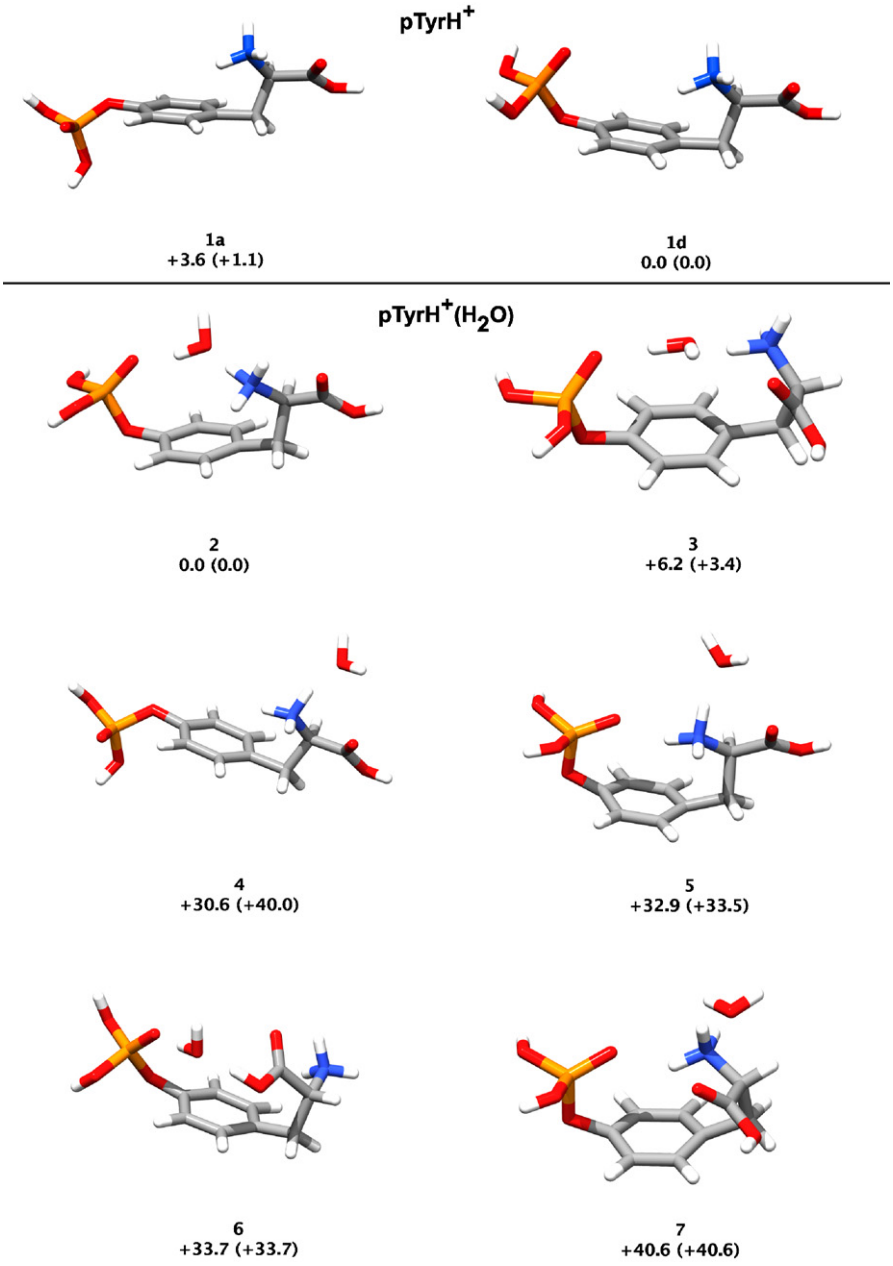

Fig. 3. Optimized structures of $pTyrH^+$ and $pTyrH^+(H_2O)$ at the MP2/SVP level. Relative free energies at 298 K, and electronic energies in parentheses, are given in kJ mol^{-1}.

water molecules involved both as donor and acceptor of hydrogen bonds.

Upon forming a hydrogen bond, ammonium NH stretches tend to broaden and shift to lower frequency [28]. As recalled above, primary ammonium groups are formed in both $pTyrH^+$ and $pTyrH^+(H_2O)$, making N–H stretches indicators of possible differences in ammonium environments. In the case of $pTyrH^+(H_2O)$, a broad feature is observed around 2750 cm^{-1}. This band is a typical signature of hydrogen bonded NH stretching vibration. On the other hand, $pTyrH^+$ has a much sharper band (fwhm = 35 cm^{-1}) centered at 3343 cm^{-1} which is likely to be the signature of a free ammonium NH stretch. The large red-shift (−600 cm^{-1}) associated with the broad feature of $pTyrH^+(H_2O)$ at 2750 cm^{-1} is thus the signature of a strong hydrogen bond involving the ammonium as a donor.

As discussed in details in the following sections, intramolecular hydrogen bonding interactions in protonated tyrosine and phospho-tyrosine are very similar. Hydrogen bonded NH stretching frequencies for protonated tyrosine were found to range from ∼3050 to ∼3150 cm^{-1} [14]. It is therefore likely that the broad band observed between 3060 and 3260 cm^{-1} in the IR spectrum of $pTyrH^+$ is the signature of hydrogen bonded NH stretches. Compared to the large red-shift discussed above for $pTyrH^+(H_2O)$, the smaller shift observed in the case of $pTyrH^+$ seems to confirm our conclusions based on our mid-IR spectrum of protonated phospho-tyrosine [11]: due to phenyl ring spacer, the strength of intramolecular hydrogen bonding between the ammonium and phosphate group is weak.

As can be seen in Fig. 2, the lower frequency region of the IR spectrum of $pTyrH^+(H_2O)$ is relatively rich. This is likely to be due to the fact that this ion has a low energy fragmentation threshold. One can observe weak and relatively sharp IR bands at 2950 and 3050 cm^{-1}, and at higher frequencies a broad feature observed between 3060 and 3460 cm^{-1}. On the blue-side of this broad band, one would expect a contribution from free NH stretches which

are observed at 3343 cm^{-1} for $pTyrH^+$, while hydrogen bonded NH stretch would contribute to the red-side. Nevertheless, as discussed above, the water molecule could be involved as a hydrogen bond donor and acceptor, and based on the literature [28], the corresponding hydrogen bonded water OH stretching frequency should be about 3300 cm^{-1}.

As a conclusion, the experimental spectrum of $pTyrH^+(H_2O)$ is structured enough that taking advantage of previously published work enables deciphering some of the main structural features of this ion. Full band assignment and precise translation into one or several structures requires the help of modeling, which is described in the next section.

3.2. Structures and spectral assignments

3.2.1. Protonated phospho-tyrosine $pTyrH^+$

In order to assign the IR spectra of protonated tyrosine ($TyrH^+$), four low energy conformers were identified [15], all in a 3.5 kJ mol^{-1} energy window. They differ by the anti or gauche relative positions of the carboxyl and phenyl groups, and by the orientation of the phenol OH in the side chain. The same distinction is useful in $pTyrH^+$ (replacing the OH by a phosphate methyl ester), however with expected differences in relative energies. In a previously identified conformer **1a** [11], the carboxyl and phenyl groups are in the anti conformation, enabling some N–H···π interaction of one ammonium N–H on top of one phenyl carbon. The orientation of the phosphate group is such as to favor a P=O···H–C interaction with one of the nearest phenyl C–Hs. As described previously [11], there exist in addition two phosphate rotamers (named **1b** and **1c** in reference [11]), differing from **1a** by the orientations of the two POH groups, lying 0.7 and 8.7 kJ mol^{-1} higher in energy than **1a** and with similar computed IR spectra. The broadening of some of the phosphate bands in the fingerprint region was thus interpreted as resulting from a Boltzmann-weighted mixture of rotamers. This effect will not be considered further.

Another stable conformer (**1d**, see Fig. 3) which was overlooked previously is obtained when the phosphate and amino acid parts lie on the same side of the phenyl plane. This involves the same conformer as above on the amino acid side (anti carboxyl, N–H···π interaction). With respect to **1a**, the phosphate group in **1d** is rotated around the O–C bond in order to have the highly polar P=O bond point towards the ammonium. Although their distance is too large for a hydrogen bond to be established, significant stabilization may be due to electrostatic and polarization interactions. This occurs at the expense of breaking the P=O···H–C interaction in **1a**. The resulting conformer **1d** is found to lie 1.1 and 3.6 kJ mol^{-1} lower than **1a** in energy and free energy, respectively. Thus a mixture with significant populations of conformers **1a** and **1d** could be expected to be present under our experimental conditions. As said above, structure **1d** was overlooked previously. Nevertheless, the computed IR absorption spectra for these two **1a** and **1d** structures are so similar that they cannot be distinguished based on the IRMPD spectrum. A mixture would only contribute to slight band broadening.

3.2.2. Hydrated, protonated phospho-tyrosine $pTyrH^+(H_2O)$

When a water molecule is attached to $pTyrH^+$, it is expected to bind to the ammonium group in order to form a strong ionic hydrogen bond. In addition, H_2O may bridge between the ammonium and either the carboxyl or the phosphate groups. This possibility is consistent with the previous discussion of the OPO spectrum, which led to the conclusion that H_2O could be both donor and acceptor of hydrogen bonds. All of these structural types were taken into account in a computational search of the $pTyrH^+(H_2O)$ potential energy surface, leading to six conformers located on the MP2/SVP surface. They are displayed in Fig. 3, together with their relative energies and free energies. We find that the most stable structures, named **2** and **3**, have the water molecule bridging between the ammonium and the phosphate. In both, H_2O is an acceptor from N–H and a donor to O=P. In addition, it is a donor to O=C in **3**. There is one N–H···O=C interaction in both, however the H···O distances (2.083 and 2.619 Å in **2** and **3**, respectively) suggest that it is stronger in **2**. Another difference is the existence of a weak N–H π interaction in **2** while the third ammonium N–H is free in **3**. Structure **2** is found to be more stable than **3** by 3.4 and 6.2 kJ mol^{-1} in energy and free energy at 298 K, respectively. Thus a mixture of both may be present with the experimental conditions used. Such structures are significantly constrained by their network of hydrogen bonds. Other structures are much less stable, by 30–40 kJ mol^{-1} in free energy. Structures **4**–**7** do not have H_2O bridging between the amino acid and the phosphate. Their less constrained structures make them more favorable entropically, however the enthalpy penalty is strong enough that they can be discarded. Structure **5** is analogous to structure **1d** of $pTyrH^+$ with a direct phosphate–ammonium interaction; its high energy in $pTyrH^+(H_2O)$ illustrates the large stabilization brought by water bridging between the phosphate and the ammonium.

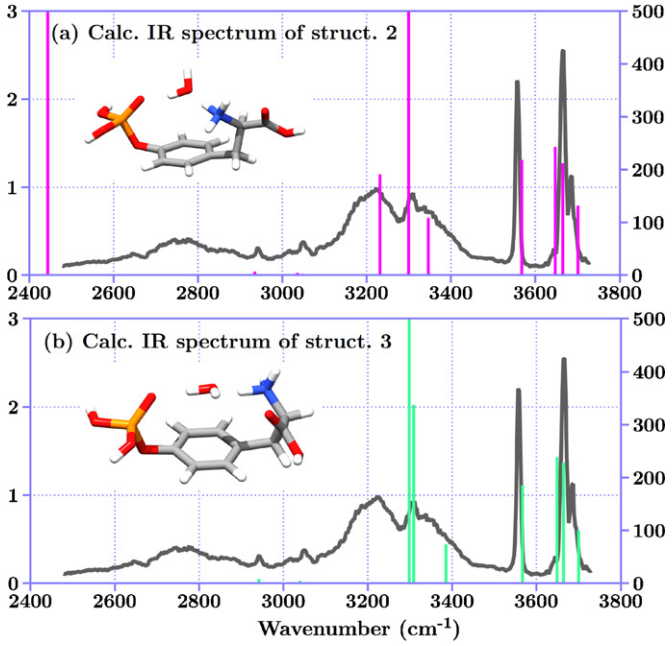

Fig. 4. IR spectra of $pTyrH^+(H_2O)$ in the 2400–3700 cm^{-1} region. The stick bars represent the calculated intensities (right ordinate in km mol^{-1}) for structures **2** (a, top) and **3** (b, bottom) of $pTyrH^+(H_2O)$. Each calculated spectrum is superimposed with the experimental spectrum (IRMPD efficiency, left ordinate).

3.2.3. Spectral assignment in the N–H/O–H stretching region

The experimental IR photodissociation spectrum of $pTyrH^+(H_2O)$ recorded in the X–H (X = C, N, and O) stretching region is given in Fig. 4 together with the calculated IR absorption spectra of conformers **2** and **3**. As said above, the calculated harmonic frequencies were uniformly scaled by a factor of 0.943 in the 2500–3750 cm^{-1} spectral range. As can be seen in Fig. 4, the two calculated IR absorption spectra are similar in the 3500–3750 cm^{-1} region. On the other hand, they are fairly different in the NH stretching (3100–3500 cm^{-1}) region, and the experimental spectrum shows a more favorable agreement with the lowest energy conformer **2**.

An assignment of the observed IR bands of $pTyrH^+(H_2O)$ in this region is proposed in Table 1. The predicted frequencies for

Table 1
Experimental and calculated vibrational frequencies for $pTyrH^+$ and $pTyrH^+(H_2O)$ in the X–H (X = C, N, O) region. The computed frequencies were scaled by 0.943 and intensities are given in km mol^{-1}.

IRMPD	MP2/SVP	Intensity	Attribution
$pTyrH^+$			
	2935	4.0	Aliphatic C–H stretch
	3000	0.5	Aliphatic C–H stretch
	3015	0.6	Aliphatic C–H stretch
	3031	3.0	Aromatic C–H stretch
	3044	2.1	Aromatic C–H stretch
	3085	14.3	Aromatic C–H stretch
	3087	3.4	Aromatic C–H stretch
3060–3260	3123	137.4	Sym HB CO + π N–H stretch
	3222	369.0	Asym HB CO + π N–H stretch
3343	3347	146.4	Free N–H stretch
3552	3560	245.0	C–OH stretch
3667	3655	217.1	Asym P–OH stretch
	3663	239.1	Sym P–OH stretch
$pTyrH^+\cdots H_2O$			
2680–2900	2444	1749.5	H-bound water N–H stretch
2950	2935	6.4	Aliphatic C–H stretch
	2971	0.2	Aliphatic C–H stretch
	3018	0.6	Aliphatic C–H stretch
3050	3036	4.4	Aromatic C–H stretch
	3050	2.1	Aromatic C–H stretch
	3084	0.7	Aromatic C–H stretch
	3085	0.4	Aromatic C–H stretch
3223	3232	191.1	H-bound CO N–H stretch
3310	3299	775.8	H-bound water O–H stretch
3340	3346	109.0	π N–H stretch
3558	3568	218.3	C–OH stretch
3667	3647	243.1	P–OH stretch
	3665	212.5	P–OH stretch
3686	3701	131.9	Free water O–H stretch

conformer **2** support our tentative assignment of the bands observed in the 3500–3750 cm^{-1} region. The band observed at 3558 cm^{-1} corresponds to the carboxylic OH stretch, and the band at 3686 cm^{-1} to the DA water free OH stretch. Interestingly, while the width (fwhm = 12 cm^{-1}) of the band observed at 3667 cm^{-1} would suggest that the two phosphate stretches are nearly degenerate, the two corresponding frequencies are predicted to be splitted by 18 cm^{-1}. As can be seen in Fig. 4, the two small features observed at 2950 and 3050 cm^{-1} can also be safely assigned to the aliphatic and aromatic CH stretches, respectively, of the tyrosine side chain.

The calculated IR absorption spectrum of conformer **2** of $pTyrH^+(H_2O)$ between 3100 and 3500 cm^{-1} is predicted to have three strongly IR active vibrational modes. As discussed above, the ammonium in **2** is involved in a strong hydrogen bond with water, but orientation of the two other NH allow for a favorable interaction with the carboxylic CO or π-system. As a result, one NH stretch is strongly red-shifted to 2444 cm^{-1}, while two NH stretches are only slightly red-shifted (Table 1). The experimental band centered at 3223 cm^{-1} is assigned to the red-shifted NH stretching mode associated with the hydrogen bond with the carboxylic CO. The NH stretching mode associated with the hydrogen bond with the π-system is predicted to be less red-shifted (3346 cm^{-1}). Interestingly, the shape of the IR photodissociation spectrum with two maxima at ~3310 and ~3340 cm^{-1} is consistent with the fact that the red-shifted water OH stretching mode is also predicted (3299 cm^{-1}) in the same spectral range. The broad band observed between 2680 and 2900 cm^{-1} is assigned with the ammonium NH stretch associated with the hydrogen bond with water which is predicted at 2444 cm^{-1}.

As said above, structures **2** and **3** essentially differ by their IR spectrum in the 3100–3500 cm^{-1} region which is the signature of the hydrogen bonding network involving the ammonium. As can be seen in Fig. 4, conformer **3** has two nearly degenerate IR active NH and hydrogen bonded water OH stretching modes near the maximum of the IR photodissociation spectrum at ~3310 cm^{-1}. Hence, while the observed IR spectrum can be interpreted considering solely the calculated IR spectrum of the lowest energy conformer **2**, one cannot exclude that a smaller fraction of conformer **3** is populated under our experimental conditions.

In order to better substantiate the band assignment of $pTyrH^+(H_2O)$ in the NH stretching region, it is important to compare the IR photodissociation spectrum of $pTyrH^+$ with the calculated IR absorption spectrum of the lowest energy conformers. As can be seen in Fig. 5, the band observed at 3343 cm^{-1} nicely matches with the predicted wavenumber (~3347 cm^{-1}) associated with the free NH stretching mode of structure **1a**. Furthermore, the structure of the broad band with a maximum at ~3130 cm^{-1} and a shoulder on its blue-side are also consistent with the fact that conformer **1a** is predicted to have two strongly IR active NH stretching modes at 3123 and 3222 cm^{-1}. One can notice, however, that the predicted relative intensities of these two stretches associated with the hydrogen bonded NH are not consistent with the observed shape of the experimental spectrum.

A broadening of the red-shifted hydrogen bonded X–H (X = N, O) stretches is expected. Nevertheless, especially in the case of the strongly bound $pTyrH^+$ ion, one may also conceive that the broadening is further enhanced due to the large fragmentation threshold which requires the absorption of multiple photons.

This broadening may be the result of a slow heating of the ion with the OPO/OPA laser system. This laser delivers ~4 ns long pulses thus preventing absorption of multiple photons within a single pulse. This is typically evidenced by the results on $Nb^+(N_2)_n$ cluster cations [30], for example. For large n cluster sizes, the dissociation threshold was found to be low and photodissociation could be observed using an OPO/OPA laser similar to the one used here. On the contrary, IR induced fragmentation of more strongly bound small $Nb^+(N_2)_3$ clusters could not be achieved. It is worth mentioning that irradiation of the ions was performed at the turning point of a reflectron time-of-flight. As a result, the mass-selected ions can only overlap with a single ns laser pulse.

In the present case however, the $pTyrH^+$ ions are stored in a Penning-ion trap where they are irradiated for 3 s, corresponding to 75 pulses at 25 Hz. As a result, a slow multiple absorption process may occur, leading to a slow heating of the $pTyrH^+$ ions which in turn would lead to a broadening of the IR absorption bands. In order to test this hypothesis, the IR photodissociation spectrum of $pTyrH^+$ in the N–H stretching region (Fig. 6b) was also recorded using the combination of the tunable OPO/OPA laser with an auxiliary CO_2 laser (Fig. 6c). The free N–H stretching band is observed to be narrower (fwhm ~15 cm^{-1}) using the auxiliary CO_2 laser which is expected to allow for a faster rise of the ion internal energy than when only the OPO/OPA laser system is used (fwhm ~26 cm^{-1}). It thus seems to confirm that the spectroscopy in the N–H stretching region of strongly bound ions such as $pTyrH^+$ may require the use of auxiliary CO_2 laser to limit band broadening. The lower energy part of the CO_2–OPO/OPA spectrum (Fig. 6b) may be more structured. However the small fragmentation efficiency using short irradiation of 500 ms precludes definitive conclusions.

An additional IR photodissociation spectrum was recorded in the NH stretching region, and the benzyl ammonium $C_6H_5CH_2NH_3^+$ ion was chosen. This system is relevant because it has a low dissociation threshold, and because its ammonium group cannot be involved in hydrogen bonding. As can be seen in Fig. 6, the signal-to-noise is too low to clearly distinguish the band (~3240 cm^{-1}) corresponding to the symmetric ammonium N–H stretching mode predicted at 3232 cm^{-1}. On the other hand, the nearly degenerate asymmetric N–H combinations predicted at 3348 cm^{-1} can clearly be observed at 3328 cm^{-1}. The position of this band (3328 cm^{-1}) falls in the typical frequency range where free ammonium N–H

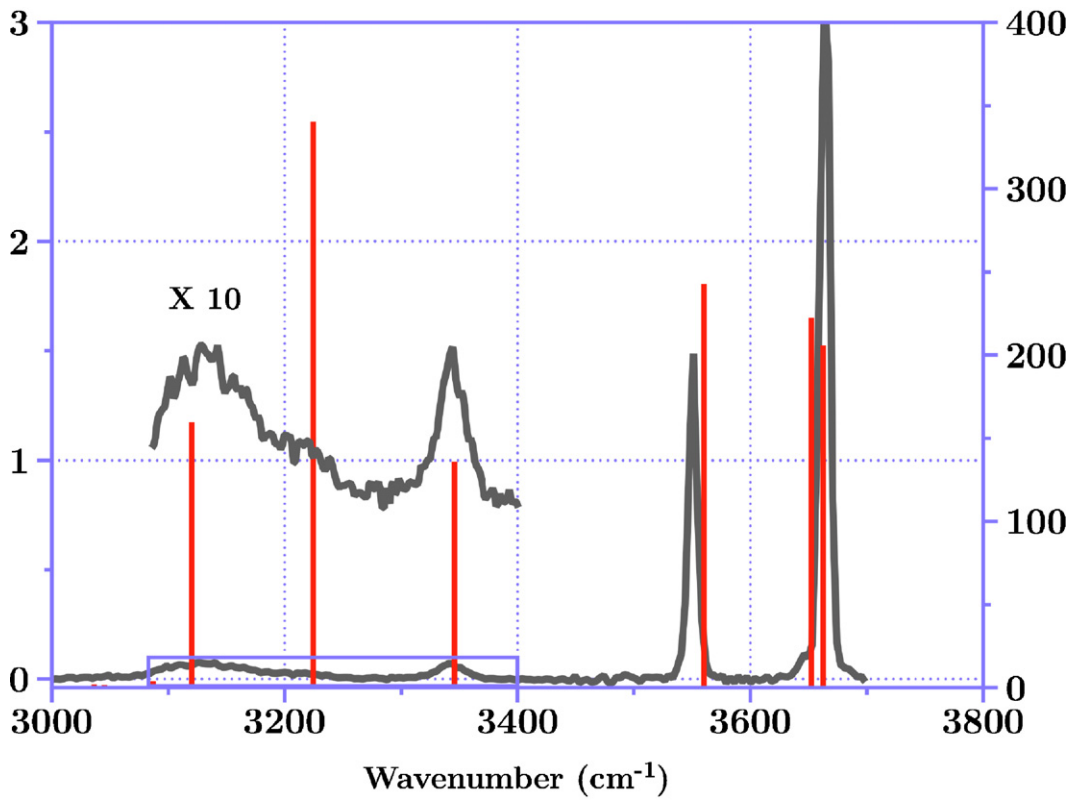

Fig. 5. IR spectra of $pTyrH^+$ in the 2400–3700 cm^{-1} region. The stick bars represent the calculated intensities (right ordinate in km mol^{-1}) for structure **1a** of $pTyrH^+$ which is superimposed with the experimental spectrum (IRMPD efficiency, left ordinate).

stretches are expected since, for instance, symmetric and asymmetric N–H stretching modes of free NH_4^+ were reported at 3270 and 3343 cm^{-1} respectively [31]. Unfortunately, the band associated with the symmetric stretch is poorly defined. The fwhm (~22 cm^{-1}) can only be characterized for the band at 3328 cm^{-1} associated with the two nearly degenerate asymmetric N–H stretches. It is slightly sharper than the free NH stretch band (fhwm ~26 cm^{-1}) of the more strongly bound $pTyrH^+$ ion suggests that multiphotonic effects may contribute to broadening of the IR photodissociation bands of $pTyrH^+$.

3.2.4. Comparison of MP2 and DFT computed spectra for structure **2**

To discuss the performance of DFT to reproduce the IRMPD spectrum of $pTyrH^+(H_2O)$, the superposition of IRMPD and DFT spectra for conformer **2**, using both B3LYP-D and M06 functionals, is given in supplementary material (see Fig. S1). As for MP2 spectra, the calculated frequencies were scaled uniformly in the X–H (X = C, N, O) stretching region. The standard scaling factor of 0.96 was used for the B3LYP-D frequencies [32]. A scaling factor of 0.94 was applied at the DFT/M06 level to reproduce experiments for the free O–H stretching modes. As for MP2 results, the DFT calculations are able to reproduce the spectrum in the 3500–3750 cm^{-1} region corresponding to free water, phosphate and carboxylic OH stretches. However, the positions of the three bands between 3100 and 3500 cm^{-1} are quite different according to the functional. B3LYP-D results are very similar to the MP2 ones with red-shifted NH stretching modes calculated at 3344 and 3233 cm^{-1} for the NH involved in the π-interaction and the hydrogen bond with carboxylic CO. On the contrary, the M06 functional predicts these modes at 3289 (π-interaction) and 3158 cm^{-1} (CO-interaction). Furthermore, the major difference concerns the red-shifted water OH stretch which is predicted at 3188 cm^{-1} at B3LYP-D level and 3353 cm^{-1} at M06 level. As for MP2 results, the frequency attributed to the ammonium NH stretch involved in the hydrogen bond with water, corresponding to the broad band between 2680 and 2900 cm^{-1}, is calculated with a too large a red-shift (2326 and 2569 cm^{-1} at the B3LYP-D and M06 levels, respectively). Comparison of the present DFT and MP2 results adds to previous results in the literature [32] in indicating that it is still difficult to find an appropriate density functional to reproduce the stretching frequencies of NH and OH groups involved in hydrogen bonds.

3.2.5. Spectral assignment in the fingerprint region

The above analysis of the IR spectrum of $pTyrH^+(H_2O)$ in the 2500–3750 cm^{-1} spectral range is consistent with theory which predicts the lowest energy structure (**1**) to involve a water molecule forming a hydrogen bonded bridge between the P=O and the ammonium groups. In order to assess the effect of the addition of water on protonated phospho-tyrosine, the IR fingerprint spectra of $pTyrH^+$ and of $pTyrH^+(H_2O)$ are superimposed in the upper part of Fig. 7 (chart a). In the lower part of this Figure, the IRMPD spectrum of $pTyrH^+(H_2O)$ is compared against the calculated MP2 spectrum of structure **2**.

A uniform scaling factor (0.96) has been applied to all MP2 calculated harmonic frequencies. It should be stressed that a detailed study of 900 vibration modes of 111 individual molecules with available IR frequencies showed that an average absolute deviation of 30 cm^{-1} can be expected at the MP2 level using a polarized TZ basis set [33]. In the present case, while the calculated CO stretching scaled value (1799 cm^{-1}) is overestimated as compared with the experimental value (1756 cm^{-1}), there is a good correspondence between all other experimental bands and predicted IR active modes of conformer **2**. This allows for a clear assignment of the various bands observed for $pTyrH^+(H_2O)$ including their frequency

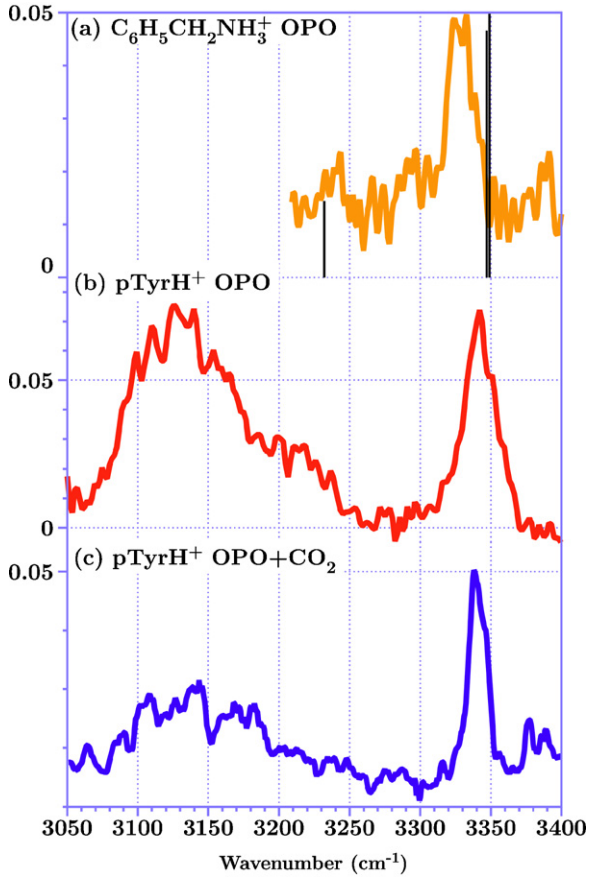

Fig. 6. IR spectra in the N–H stretching region of $C_6H_5CH_2NH_3^+$ (a, top) and pTyrH$^+$ (b, middle and c, bottom). Spectra in (a) and (b) have been recorded using the OPO/OPA laser only. The spectrum in (c) has been recorded using the combination of OPO/OPA and auxiliary CO_2 lasers. In (a) the experimental spectra (IRMPD efficiency, left ordinate) are superimposed with calculated MP2 stick bar spectra.

Table 2
Experimental and calculated vibrational frequencies for pTyrH$^+$(H_2O) in the 800–1900 cm^{-1} region. The computed frequencies were scaled by 0.96 and intensities are given in km mol^{-1}.

IRMPD	MP2/SVP	Intensity	Attribution
pTyrH$^+$···H_2O			
	864	12.5	P–OH stretch
	890	15.4	Aromatic C–H bend out of plane
	902	242.6	POH bend, P–OH stretch
930	913	505.2	POH bend, P–OH stretch, P–O(C) stretch
	918	57.2	Aromatic C–H bend out of plane
	922	18.5	Aromatic C–H bend out of plane
	953	12.1	C–C stretch, NH_3 torsion, C–H bend
	969	161.8	POH bend
	990	5.5	Aromatic C–H bend
1004	1000	121.1	POH bend
	1067	4.6	C–H bend, aromatic C–H bend
	1087	36.4	Aromatic C–H bend
	1092	24.3	C–H bend, NH_3 torsion
	1119	11.5	C–H bend, NH_3 torsion
	1141	9.8	Aromatic C–H bend
1157	1169	202.9	C–OH bend (C–OH stretch) out of phase
	1194	4.6	C–H bend, aromatic C–H bend
1223	1225	11.4	C–H bend, C–OH bend, NH_3 torsion
	1228	122.5	O(P)–C stretch, aromatic C–H bend, C–H bend
	1252	12.2	C–H bend
	1271	1.6	Aromatic C–H bend
1283	1279	362.9	P=O stretch
	1316	7.8	C–H bend
	1337	4.3	C–H bend
	1395	1.8	C=C stretch, aromatic C–H bend, C–H bend
1380	1409	119.3	(C–OH bend), C–OH stretch in phase
	1427	23.2	C–H bend
	1440	1.5	C=C stretch, aromatic C–H bend
1490	1493	121.8	NH_3 umbrella
	1498	128.3	Aromatic C–H bend, NH_3 umbrella
1550–1651	1573	48.9	NH_3 scissor, H_2O bend
	1593	2.9	C=C stretch
	1620	25.2	C=C stretch
	1637	33.1	NH_3 scissor, H_2O bend
	1658	53.3	NH_3 scissor, H_2O bend
1756	1799	227.5	C=O stretch, COH bend

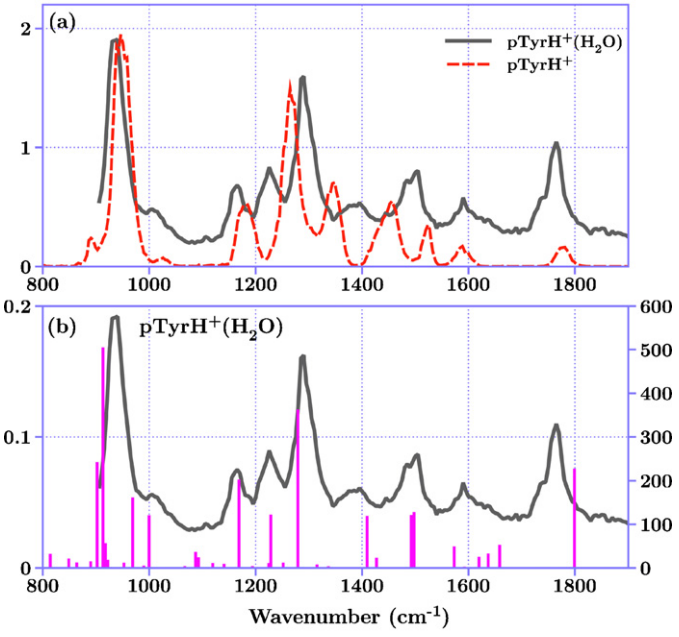

Fig. 7. IR photodissociation spectra of pTyrH$^+$(H_2O) and pTyrH$^+$ recorded in the 800–1900 cm^{-1} region. In chart (a), the two experimental spectra are superimposed. In chart (b), the calculated and experimental spectra of pTyrH$^+$(H_2O) are superimposed. Experimental IRMPD efficiency scales are on the left ordinate, computed absorption efficiency scale is on the right ordinate.

shifts induced by the hydrogen bonds associated with the water bridge.

The intense band at 1283 cm^{-1} can be safely assigned to the P=O stretching mode which is predicted at 1279 cm^{-1}. As discussed in our previous IR fingerprint study of protonated phosphorylated amino acids, in contrast to pSerH$^+$ and pThrH$^+$, the aromatic ring spacer prevents the charge solvation of the ammonium by the P=O group which can thus be considered as "free" in pTyrH$^+$. The red-shift of −65 cm^{-1} of the P=O stretching mode when adding the water molecule to pTyrH$^+$ is thus consistent with structure **2** since the hydrogen bond with water is expected to weaken the P=O bond.

The bridging water molecule also makes a hydrogen bond with the ammonium. The comparison of the IR fingerprint spectra of pSerH$^+$ and pThrH$^+$ with that of pTyrH$^+$ showed that the umbrella mode of ammonium is very sensitive to hydrogen bonding [11]. In the case of pTyrH$^+$(H_2O), it is observed at 1490 cm^{-1}. The blue shift of ~30 cm^{-1} with respect to pTyrH$^+$ (characterized by a nearly free P=O stretch at 1460 cm^{-1}) is also consistent with structure **2** since it is a consequence of the constrain imposed by the hydrogen bond to the ammonium. Interestingly, the frequency shift is smaller than for pSerH$^+$ and pThrH$^+$ (~70 cm^{-1}). It thus seems that the intramolecular P=O···ammonium hydrogen bond is stronger than the water–ammonium hydrogen bond in the case of pTyrH$^+$(H_2O). The asymmetric deformation of the ammonium group should also be affected by the hydrogen bond. Unfortunately, it falls in a spectral region where other IR active modes (C=C stretch, water bending) contribute to the IR cross section. In the case of pTyrH$^+$(H_2O), it gives rise to a broad band between 1550 and 1650 cm^{-1}.

An assignment of the main IR fingerprint bands of $pTyrH^+(H_2O)$ is proposed in Table 2. As can be seen in this table, the O(P)–C stretch observed at 1533 cm^{-1} for $pTyrH^+(H_2O)$ seems to be sensitive to the hydrogen bond of the phosphate with water. Compared to $pTyrH^+$, the red-shift of $\sim$–42 cm^{-1} can be attributed to the electronic reorganization of the phosphate associated with the formation of the hydrogen bond with water. This red-shift is slightly underestimated (−28 cm^{-1}) at the MP2 level.

4. Conclusions

Infrared spectra of mono-hydrated protonated phospho-tyrosine $pTyrH^+(H_2O)$ in the 900–1900 cm^{-1} and 2500–3750 cm^{-1} regions have been recorded via tunable IRMPD spectroscopy using two tunable lasers coupled with a tandem FT-ICR mass spectrometer. The effect of the addition of a water molecule on the conformational space of protonated phospho-tyrosine has been investigated using both MP2 and density functional quantum chemical calculations. This combination of tandem mass spectrometry and theory provides additional information on environment effects on the frequencies of some specific vibrational modes of the phosphate and ammonium groups. In the present case of $pTyrH^+(H_2O)$, the phosphate P═O group is involved in a strong hydrogen bond with the water molecule forming a bridge with the primary ammonium group. Theory and experimental provide compelling evidence that it results in larger frequency displacements of the IR specific structural probes than in the cases of $pSerH^+$ and $pThrH^+$ [11]. In these cases, it was found that the phosphate P═O group was a hydrogen bond acceptor from the ammonium and, conversely, the corresponding P═O stretch had been found to be red-shifted by −45 cm^{-1} with respect to its position in $pTyrH^+$ where the aromatic ring prevents for the formation of strong direct interaction between the phosphate and the ammonium. The added water molecule however forms a strong hydrogen bonded bridge in $pTyrH^+(H_2O)$ as evidenced by the larger red-shift (−65 cm^{-1}) of the P═O stretching mode.

Additional information on the effect of the phosphate group on its environment is also provided by the position of the ammonium umbrella mode. The constrain imposed by the hydrogen bond involving the ammonium results in a blue-shift of this vibrational mode. Comparison of $pTyrH^+(H_2O)$ and non-solvated $pSerH^+$ and $pThrH^+$ systems [11], suggests that the intramolecular P═O···ammonium hydrogen bond characteristic of the latter two cases is stronger than the water-ammonium hydrogen bond in the case of $pTyrH^+(H_2O)$.

Overall, the MP2 calculated IR absorption spectrum better matches with the experimental IRMPD spectrum than those obtained using density functional theory.

In the present case, the IR spectra of $pTyrH^+$ and $pTyrH^+(H_2O)$ have also been recorded in the 2500–3750 cm^{-1} spectral region. The phosphate OH stretching mode is observed at 3667 cm^{-1} for both solvated and unsolvated ions. The hydrogen bond donor–acceptor water molecule of $pTyrH^+(H_2O)$ is characterized by a band at 3686 cm^{-1} that is characteristic of the free OH stretch of such hydrogen bond donor–acceptor water molecule. The ammonium NH stretches are all red-shifted, and the extent of the red-shift reflects the strength of the three hydrogen bonds which can be formed. Consistent with a red-shift of the phosphate P═O stretch, the large red-shift of one ammonium NH stretch is the signature of a strong hydrogen bond bridge formed by water between the phosphate and the ammonium. Two other broad IRMPD bands in the spectrum of $pTyrH^+(H_2O)$ show that two weaker hydrogen interactions can take place between the ammonium and the carboxylic CO and the π-system, the former being stronger than the latter.

These results provide additional spectroscopic information on the frequency displacements of IR structure-specific modes of the phosphate group and also of other functional groups due to their environment. In particular, the phosphate P═O group is an efficient hydrogen bond acceptor, and both the P═O and the (P)C–O stretching modes appear to provide useful information on the phosphate environment.

Acknowledgements

A.S. and J.K.M. thank the vice-presidency for external relations in Ecole Polytechnique for a 1-year post-doctoral fellowship and for support from the international internship program, respectively. This work was supported by the European Commission (NEST program, Project No. 15637). The authors are grateful to J.M. Ortega and to the technical support at the CLIO facility. This work was granted access to the HPC resources of [CCRT/CINES/IDRIS] under the allocation x2011085107 made by GENCI (Grand Equipement National de Calcul Intensif).

Appendix A. Supplementary data

Supplementary data associated with this article can be found, in the online version, at doi:10.1016/j.ijms.2011.08.031.

References

[1] F. Diella, S. Cameron, C. Gemund, R. Linding, A. Via, B. Kuster, T. Sicheritz-Ponten, N. Blom, T.J. Gibson, BMC Bioinformatics 5 (2004) 79–83;
A. Kreegipuu, N. Blom, S. Brunak, Nucleic Acids Res. 27 (1999) 237–239;
N. Blom, A. Kreegipuu, S. Brunak, Nucleic Acids Res. 26 (1998) 382–386.
[2] L.N. Johnson, R.J. Lewis, Chem. Rev. 101 (2001) 2209–2242.
[3] M.J. Chalmers, W. Kolch, M.R. Emmett, A.G. Marshall, H. Mischak, J. Chromatogr. B Analyt. Technol. Biomed. Life Sci. 803 (2004) 111–120;
C. Stingl, C. Ihling, G. Ammerer, A. Sinz, K. Mechtler, Biochim. Biophys. Acta Proteins Proteomics 1764 (2006) 1842–1852;
C.M. Spickett, A.R. Pitt, N. Morrice, W. Kolch, Biochim. Biophys. Acta Proteins Proteomics 1764 (2006) 1823–1841.
[4] S.A. Carr, M.J. Huddleston, R.S. Annan, Anal. Biochem. 239 (1996) 180–192;
M.J. Huddleston, R.S. Annan, M.F. Bean, S.A. Carr, J. Am. Soc. Mass. Spectrom. 4 (1993) 710–717.
[5] J.W. Flora, D.C. Muddiman, J. Am. Soc. Mass. Spectrom. 15 (2004) 121–127;
J.W. Flora, D.C. Muddiman, J. Am. Chem. Soc. 124 (2002) 6546–6547;
J.W. Flora, D.C. Muddiman, Anal. Chem. 73 (2001) 3305–3311.
[6] M.C. Crowe, J.S. Brodbelt, Anal. Chem. 77 (2005) 5726–5734;
M.C. Crowe, J.S. Brodbelt, J. Am. Soc. Mass. Spectrom. 15 (2004) 1581–1592.
[7] J. Oomens, B.G. Sartakov, G. Meijer, G. Von Helden, Int. J. Mass Spectrom. 254 (2006) 1–19;
J. Oomens, A.J.A. van Roij, G. Meijer, G. von Helden, Astrophys. J. 542 (2000) 404–410;
J. Lemaire, P. Boissel, M. Heninger, G. Mauclaire, G. Bellec, H. Mestdagh, A. Simon, S.L. Caer, J.M. Ortega, F. Glotin, P. Maitre, Phys. Rev. Lett. 89 (2002) 273002;
P. Maitre, S. Le Caer, A. Simon, W. Jones, J. Lemaire, H.N. Mestdagh, M. Heninger, G. Mauclaire, P. Boissel, R. Prazeres, F. Glotin, J.M. Ortega, Nucl. Instrum. Methods Phys. Res. Sect. A 507 (2003) 541–546.
[8] J.M. Bakker, T. Besson, J. Lemaire, D. Scuderi, P. Maitre, J. Phys. Chem. A 111 (2007) 13415–13424.
[9] N.C. Polfer, J.J. Valle, D.T. Moore, J. Oomens, J.R. Eyler, B. Bendiak, Anal. Chem. 78 (2006) 670–679.
[10] O.P. Balaj, C. Kapota, J. Lemaire, G. Ohanessian, Int. J. Mass Spectrom. 269 (2008) 196–209.
[11] C.F. Correia, P.O. Balaj, D. Scuderi, P. Maitre, G. Ohanessian, J. Am. Chem. Soc. 130 (2008) 3359–3370.
[12] D. Scuderi, C.F. Correia, O.P. Balaj, G. Ohanessian, J. Lemaire, P. Maitre, Chemphyschem 10 (2009) 1630–1641;
A. Cimas, P. Maitre, G. Ohanessian, M.P. Gaigeot, J. Chem. Theory Comput. 5 (2009) 2388–2400.
[13] C.F. Correia, C. Clavaguera, U. Erlekam, D. Scuderi, G. Ohanessian, Chemphyschem 9 (2008) 2564–2573.
[14] J.A. Stearns, S. Mercier, C. Seaiby, M. Guidi, O.V. Boyarkin, T.R. Rizzo, J. Am. Chem. Soc. 129 (2007) 11814–11820.
[15] J.A. Stearns, M. Guidi, O.V. Boyarkin, T.R. Rizzo, J. Chem. Phys. 127 (2007) 154322.
[16] A. Kamariotis, O.V. Boyarkin, S.R. Mercier, R.D. Beck, M.F. Bush, E.R. Williams, T.R. Rizzo, J. Am. Chem. Soc. 128 (2006) 905–916.
[17] J.M. Bakker, R.K. Sinha, T. Besson, M. Brugnara, P. Tosi, J.Y. Salpin, P. Maitre, J. Phys. Chem. A 112 (2008) 12393–12400.

[18] J.M. Bakker, J.Y. Salpin, P. Maitre, Int. J. Mass Spectrom. 283 (2009) 214–221.
[19] R.K. Sinha, E. Nicol, V. Steinmetz, P. Maitre, J. Am. Soc. Mass. Spectrom. 21 (2010) 758–772.
[20] R. Prazeres, F. Glotin, C. Insa, D.A. Jaroszynski, J.M. Ortega, Eur. Phys. J. D: Atom. Mol. Opt. Phys. 3 (1998) 87–93.
[21] D. Semrouni, O.P. Balaj, F. Calvo, C.F. Correia, C. Clavaguera, G. Ohanessian, J. Am. Soc. Mass. Spectrom. 21 (2010) 728–738.
[22] S. Grimme, J. Comput. Chem. 27 (2006) 1787–1799;
A.D. Becke, J. Chem. Phys. 98 (1993) 5648–5652.
[23] Y. Zhao, D.G. Truhlar, Theor. Chem. Acc. 120 (2008) 215–241.
[24] M.J. Frisch, Gaussian 09, Revision B. 01, Gaussian, Inc, Wallingford, CT, 2009.
[25] R. Ahlrichs, M. Bar, M. Haser, H. Horn, C. Kolmel, Chem. Phys. Lett. 162 (1989) 165–169, for the current version, see: http://www.turbomole.com.
[26] F. Rogalewicz, Y. Hoppilliard, G. Ohanessian, Int. J. Mass Spectrom. 196 (2000) 565.
[27] R. Withnall, L. Andrews, J. Phys. Chem. 91 (1987) 784–797.
[28] H.C. Chang, Y.S. Wang, Y.T. Lee, H.C. Chang, Int. J. Mass Spectrom. 180 (1998) 91–102.
[29] E.G. Diken, N.I. Hammer, M.A. Johnson, R.A. Christie, K.D. Jordan, J. Chem. Phys. 123 (2005).
[30] E.D. Pillai, T.D. Jaeger, M.A. Duncan, J. Am. Chem. Soc. 129 (2007) 2297–2307.
[31] C.S. Gudeman, R.J. Saykally, Annu. Rev. Phys. Chem. 35 (1984) 387–418.
[32] D. Semrouni, C. Clavaguera, J.P. Dognon, G. Ohanessian, Int. J. Mass Spectrom. 297 (2010) 152–161.
[33] M.D. Halls, J. Velkovski, H.B. Schlegel, Theor. Chem. Acc. 105 (2001) 413–421.